Microporous Silicates

DOI: 10.1002/anie.200704222

A Multi-Dimensional Microporous Silicate That Is Isomorphous to Zeolite MCM-68**

*Yoshihito Koyama, Takuji Ikeda, Takashi Tatsumi, and Yoshihiro Kubota**

Zeolites with large pores and multi-dimensional channel systems allow the diffusion of large molecules inside the pores. The number of zeolites with such characteristics is still limited, however, therefore the synthesis of new large-pore, multi-dimensional zeolites remains important. MCM-68 (MSE topology[1]) is a new type of multi-dimensional zeolite with a $12\times10\times10$-membered ring (MR) pore system where a 12-MR straight channel intersects with two independent twisted 10-MR channels. This material also contains a supercage (18×12-MR) that is accessible only through the 10-MR pores. The synthesis and structural elucidation of this zeolite was first achieved by researchers from Mobil,[2,3] and various applications, such as alkylation catalysts[4] and hydrocarbon traps,[5] have been reported independently since then.

To date this zeolite has only been synthesized under hydrothermal conditions by using *N*,*N*,*N*′,*N*′-tetraethylbicyclo[2.2.2]oct-7-ene-2,3:5,6-dipyrrolidinium diiodide ($TEBOP^{2+}(I^-)_2$), which is a derivative of bicyclo[2.2.2]oct-7-ene-2,3:5,6-tetracarboxylic dianhydride (BOTD), as an organic structure-directing agent (SDA). The gel-composition window for the successful crystallization of pure MCM-68 is very narrow and the Si/Al ratio of the product is limited to 9–12.[2,3] Alteration of the chemical composition of the product by direct crystallization is therefore difficult to carry out.[6]

In the course of our studies aimed at improving this synthetic method, we found that use of the "steam-assisted crystallization"[7] (SAC) method gives a highly crystalline MSE analogue with a previously unattainable chemical composition, namely a purely siliceous composition, that is totally different from that of a typical MCM-68. Unlike the starting gel for MCM-68, which contains K^+ and $TEBOP^{2+}(I^-)_2$), our gel has a more ordinary, halogen-free composition (containing Na^+ as well as the dihydroxide form of $TEBOP^{2+}$). Moreover, the crystallization period is much shorter (5 days at 150 °C) than for MCM-68 (16 days at 160 °C).

The as-synthesized crystalline material was found to be a composite of the SDA and to have an incomplete MSE framework owing to a significant number of defects (vacant sites). Although the composite does not retain its structure upon removal of the SDA, filling the vacant sites with atoms from external sources in a post-synthesis treatment provided the material with robustness. This result indicates that the as-synthesized material containing defects could be a potential precursor of various metallosilicate analogues of MSE-type materials. We designate this precursor material as YNU (Yokohama National University)-2P and the corresponding SDA-free material obtained after the post-synthetic treatment as YNU-2. YNU-2 is the first example of a highly crystalline, pure-silica version of an MSE-like molecular sieve. We report herein the synthesis and structural analysis of YNU-2P and YNU-2.

The dihydroxide form $TEBOP^{2+}(OH^-)_2$ was synthesized from the corresponding diiodide with an overall yield starting from commercially available BOTD of 59%. Synthesis of the molecular sieve was carried out under SAC conditions with $TEBOP^{2+}(OH^-)_2$. The as-synthesized product (YNU-2P) was analyzed mainly by powder X-ray diffraction (XRD) as well as ^{29}Si magic-angle spinning (MAS) NMR spectroscopy. The detailed synthetic procedure and analytical methods are described in the Experimental Section.

As described above, removal of the SDA from YNU-2P by calcination caused the framework to collapse. However, post-synthesis silylation was found to be effective in avoiding this collapse (see the Supporting Information). This method consists of treating the as-synthesized sample with tetramethyl orthosilicate (TMOS) vapor and conc. HCl vapor in an autoclave, followed by heating statically at 170 °C for 24 h. The resultant crystalline structure was retained after removal of the SDA by calcination in air at 450–600 °C. It is noteworthy that the silylation occurs in both the vapor and liquid phases. The resultant highly crystalline microporous silicate (YNU-2) was analyzed in the same way as YNU-2P.

A careful structural analysis allowed us to explain this synthetic behavior. The initial lattice constants of YNU-2P were determined to be $a=1.8268$ and $c=2.0071$ nm by an indexing procedure using the program DICVOL06.[8] The most probable space group (centrosymmetric $P4_2/mnm$), as

[*] Y. Koyama, Prof. Y. Kubota
Division of Materials Science and Chemical Engineering
Graduate School of Engineering
Yokohama National University
79-5 Tokiwadai, Hodogaya-ku, Yokohama 240-8501 (Japan)
Fax: (+81) 45-339-3926
E-mail: kubota@ynu.ac.jp
Dr. T. Ikeda
Research Center for Compact Chemical Process
National Institute of Advanced Industrial Science and Technology
AIST Tohoku
Technology, AIST Tohoku
4-2-1 Nigatake, Miyagino-ku, Sendai, 983-8551 (Japan)
Prof. T. Tatsumi
Chemical Resources Laboratory
Tokyo Institute of Technology
Nagatsuta 4259, Midori-ku, Yokohama 226-8503 (Japan)

[**] This work was partly supported by the Core Research for Evolutional Science and Technology (CREST) program of JST Corporation. T.I. thanks MEXT KAKENHI (18760513) for supporting the structural part of this work.

Supporting information for this article is available on the WWW under http://www.angewandte.org or from the author.

determined from the reflection conditions, is consistent with that of calcined MCM-68.[1] Detailed crystallographic information is summarized in Table 1. The integral intensities for each reflection were extracted by the Le Bail method using

Table 1: Experimental XRD conditions and crystallographic data for YNU-2P and YNU-2.[a]

	YNU-2P	YNU-2
refined chemical formula	$Na_{12.2}Si_{98.3}O_{202.7}$ ·4[TEBOP(OH)$_2$]·21.9 (H_2O)	$Si_{111.6}O_{224}$·22.7 H_2O
F_W	7977.5	6730.08
space group	$P4_2/mnm$ (no. 136)	$P4_2/mnm$ (no. 136)
a [nm]	1.826850(5)	1.82222(2)
c [nm]	2.007065(7)	2.00401(2)
unit-cell volume [nm^3]	6.69834(4)	6.65431(12)
profile range in FWHM	12	12
FWHM [°]	0.075 (at 2θ = 8.8°)	0.083 (at 2θ = 8.2°)
number of observations	10876	10876
number of contributing reflections	1895	1886
number of refined structural parameters	105	92
R_{wp} (Rietveld)	0.0318	0.0332
R_F (Rietveld)	0.0263	0.0056
R_e (Rietveld)	0.0247	0.0378
χ^2	3.7	0.8

[a] $Cu_{K\alpha1}$ radiation; 2θ = 5–100°, step size (2θ): 0.0087115°, counting time per step: 40 s.

the program RIETAN-FP.[9] An initial structure model was obtained by the powder charge flipping (*pCF*)[10] method with histogram matching using the program Superflip[11] as the *pCF* method has been shown to be very useful for solving microporous structures.[10,12] This *pCF* analysis showed the structure of YNU-2P to have an MSE-type framework composed of eight T-sites and nineteen O-sites.[1] The initial structural model was refined by the Rietveld method using RIETAN-FP. The distributions of guest atoms, molecules, and organic cations were estimated by an electron density distribution calculated from a combination of maximum entropy (MEM) and Rietveld methods.[13] The MEM analysis was conducted by using the program PRIMA.[14] Finally, the structural model was further refined by an MEM-based pattern fitting (MPF) method[15] at the electron-density level. The crystal structural models and electron-density distributions were visualized with the VENUS package.[16]

In the first stage, the position of the $TEBOP^{2+}$ ion in YNU-2P was estimated by optimizing the simple coulomb interaction between the framework atoms and organic guests. The gravity points of the $TEBOP^{2+}$ ions were then set to (0,0,1/2) in the super-cage and (1/2,0,1/2) in the straight channel. A split-atom model was adopted for the $TEBOP^{2+}$ cations in the super-cage and the straight channel during the refinement, although the atomic coordinates were fixed to decrease the correlation with these parameters. In addition, a number of OH^- anions and adsorbed water molecules were detected near $TEBOP^{2+}$ ions in the cages. The distribution of water and $TEBOP^{2+}$ cations in the straight channel is highly disordered. Two Na^+ sites are observed in the $6^25^44^2$ cage and one in an elliptical 8-MR. This refinement based on the preliminary model converged poorly ($R_F \approx 8.5\,\%$) and showed large distortions of the framework atoms with inadequate Si–O bond lengths.

This analytical result suggests that a long-range ordering of Si atom defects might have occurred in the framework. The Si atom defects were therefore recognized by refining the occupancy factors, g, for all T-sites. The refined g values of four tetrahedral sites (T1, T3, T6, and T7) are remarkably low (approx. 0.84, 0.90, 0.40, and 0.40, respectively), whereas the rest of the T-sites are fully occupied, as shown in Figure 1. Si atom defects on the both T6 and T7, therefore, should occur simultaneously. These four T-sites are incorporated into the complex building unit composed of three kinds of simple building units ($6^25^44^2$, 5^44^3, and 5^4). The refinement of g(O) suggests the existence of defective oxygen sites that bond to defective T-sites as described above. As a result, the chemical composition of the framework was estimated to be $Si_{98.3}O_{204.7}$, which indicates that the molecular weight of the defective framework is about 10 % lower than that of the complete framework without defects (see the Supporting Information).

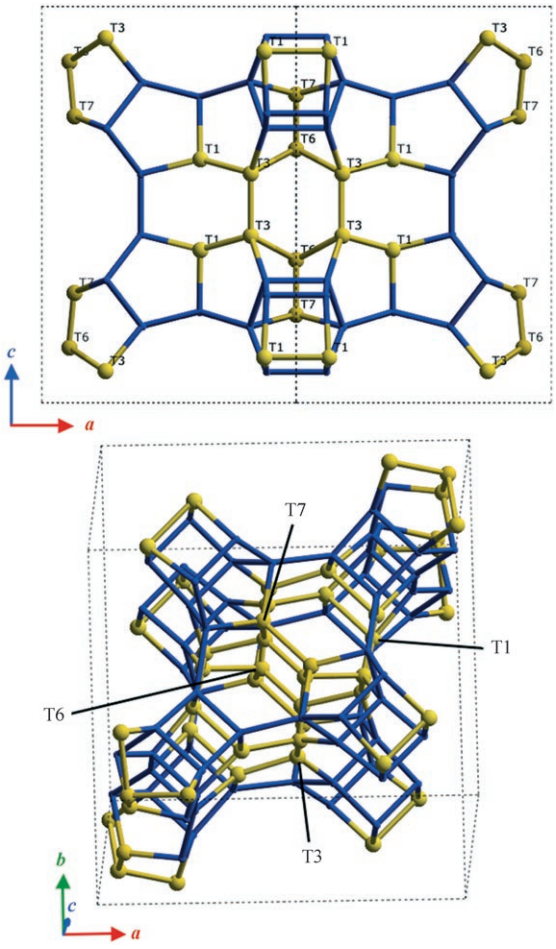

Figure 1. Representation of the framework structure of YNU-2P along the [110] (top) and [001] (bottom) directions. The yellow balls indicate defective T-sites estimated from the Rietveld refinement.

The presence of a large number of Si atom defects was confirmed by the ^{29}Si MAS NMR spectrum (Figure 2). YNU-2P exhibits resonances around $\delta = -100.7$ and -109.5 ppm that are characteristic of HO*Si*(OSi)$_3$ (Q^3) and *Si*(OSi)$_4$ (Q^4) silicon sites, respectively. The Q^3/Q^4 ratio was estimated to be

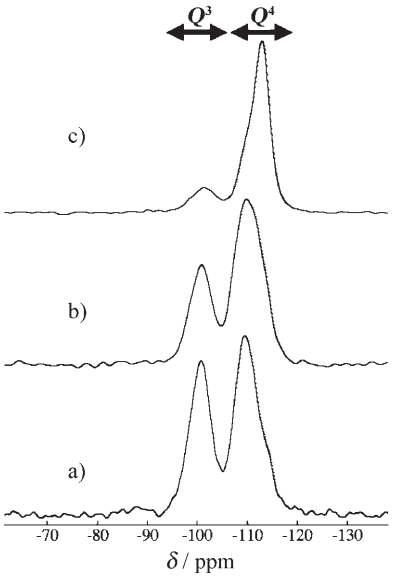

Figure 2. ^{29}Si MAS NMR spectra of a) YNU-2P, b) modified YNU-2P after post-synthesis silylation, and c) the siliceous zeolite YNU-2 formed by calcination of (b).

about 0.81, which cannot be explained without the existence of internal Si atom defects. In addition, the ^{1}H MAS NMR spectra of YNU-2P and modified YNU-2P after silylation exhibit a signal at $\delta = 15.8$ ppm arising from strong hydrogen bonding of the type $(SiO)_3Si{-}O{\cdots}H{\cdots}O{-}Si(OSi)_3$, with an O···H···O distance of 0.248 nm (cf. ref. [17]). This fact indicates that there is strong hydrogen bonding between adjacent terminal oxygen atoms around the Si atom defects. The intensity of the signal at $\delta = 15.8$ ppm for YNU-2P is decreased by the post-synthetic silylation and further decreased after calcination of silylated YNU-2P, which strongly suggests that structural defects are repaired by the post-synthetic silylation (see the Supporting Information). The final *R*-factors of YNU-2P decreased significantly to about $R_{wp} = 3.2\,\%$, $R_{Bragg} = 2.6\,\%$, and $R_F = 2.5\,\%$ when taking into account the revised structural model with Si atom defects.

The differential thermal analysis (DTA) plot of YNU-2P shows remarkable peaks for exothermic processes arising from the combustion of TEBOP^{2+} cation in the temperature range 260–600 °C. The thermogravimetric analysis (TGA) plot exhibits a large weight loss (approx. 21.4 wt %) in the same temperature range, which should correspond to organic combustion as well as the water released by a silanol condensation reaction (see the Supporting Information). The maximum number of TEBOP^{2+} cations per unit cell was assumed to be four in light of the packing density of the cation included in the framework. Based on all the above results, the chemical composition of YNU-2P was estimated to be $Na_{12.2}Si_{98.3}O_{202.7}{\cdot}4\,[TEBOP(OH)_2]{\cdot}21.9\,(H_2O)$. This Na content is consistent with that obtained by elemental analysis and suggests that Na^+ cations compensate the negative charge of the framework caused by its Si atom defects.

Figure 3 shows the electron-density distribution of YNU-2P obtained from the MPF analysis. The electron densities of the organic guests in the super-cage are considerably elongated and appear to be bone-shaped. This shape reflects that

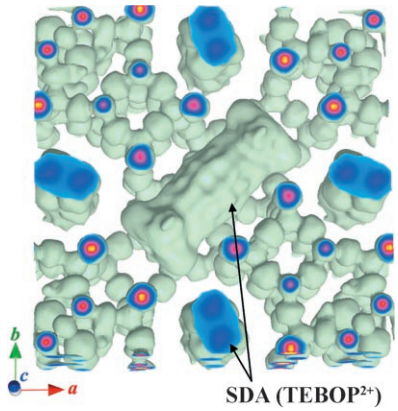

Figure 3. Electron-density distribution in YNU-2P along the [001] direction in the range $-0.25 < z < 0.14$ obtained by the MPF method. The isosurface level is set to 0.5 e Å^3.

of TEBOP^{2+} very well; the tight fit of the organic guest into the super-cage implies the strong structure-directing ability and specificity of TEBOP^{2+} cations during formation of this framework structure. The electron-density distributions of the organic guests in the 12-MR straight channel have a complicated shape—they are distributed continuously along the *c*-axis like a rod. This finding indicates that the TEBOP^{2+} cations might be randomly distributed along the *c*-axis. The electron densities of water molecules and OH^- anions are not perfectly distinguishable from those of the TEBOP^{2+} cations. No covalent bond is observed between T7 and O12 at the isosurface level of 0.5 e Å^3 owing to lattice defects, whereas bonding between other T and O sites is clearly distinguishable. The refined structural model seems to be reasonable, although the positions of the organic molecules are fixed by the simple approximation. The *R*-factors after the MPF analysis therefore decrease because of a reduced model bias in the Rietveld refinement ($R_{Bragg} = 2.6\,\% \rightarrow 1.3\,\%$ and $R_F = 2.5\,\% \rightarrow 1.4\,\%$).[15]

Structural refinement of YNU-2 showed that the Si atom defects had dramatically decreased in number, thus indicating that the Si defects are repaired by silylation. Only *g*(T6) converged to slightly less than 1.0 upon refinement of the defective site's occupancies, as was the case with YNU-2P. The presence of residual Si atom defects was also supported by the ^{29}Si DDMAS NMR spectrum shown in Figure 2, which indicates that the Q^3/Q^4 ratio has decreased. The lattice constants decrease slightly upon removing the organic guest by careful calcination after silylation (Table 1). No Na^+ cations are observed in the complex building unit, which suggests that these cations are removed by the post-synthesis

silylation under acidic conditions. Chemical analysis showed that the amount of Na was below the detection limit.

All the adsorbed water molecules (approx. 16 molecules per unit cell) were located in the 12-MR straight channel of YNU-2 at three independent sites. This amount of water molecules was supported by the TGA of YNU-2 and is consistent with an unusually hydrophilic behavior of this high-silica material. The *R*-factors converged to sufficiently low values after the Rietveld refinement. The observed, calculated, and difference patterns for YNU-2P and YNU-2 are plotted against 2θ in Figure 4.

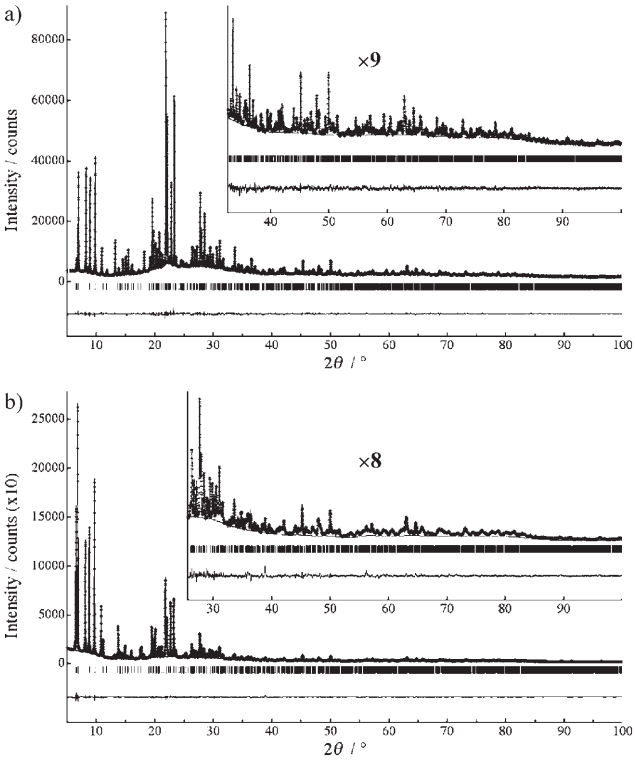

Figure 4. Difference plots of a) YNU-2P and b) YNU-2 after the Rietveld refinements. The observed diffraction intensities are represented by plus signs and the calculated pattern by the solid line. The difference between the observed and calculated intensities is plotted near the bottom. The short vertical marks below the observed and calculated patterns indicate the positions of allowed Bragg reflections.

Nitrogen adsorption/desorption measurements of YNU-2 and conventional MCM-68 gave Type-I isotherms (see the Supporting Information). The adsorption capacity for YNU-2 is 0.29 $cm^3 g^{-1}$, which is close to the value for MCM-68 (0.24 $cm^3 g^{-1}$) and suggests that the pores of YNU-2 are not blocked by amorphous silica species during the silylation process. The desorption branch of YNU-2 shows a small hysteresis, which suggests the presence of some mesopores. This adsorption behavior might not be due to the internal defects but could be related to the roughness of the outer surface of the crystal. Further investigations are therefore necessary to reach a definitive conclusion.

SEM showed that the crystal size and morphology of YNU-2 are totally different to those of MCM-68 (see the Supporting Information). The larger crystallite size of YNU-2 is one of the reasons for the sharper XRD peaks of this compound and the smaller external surface area of YNU-2 (10 $m^2 g^{-1}$) than that of MCM-68 (48 $m^2 g^{-1}$) is consistent with this difference in crystallite size.

In summary, a new type of crystalline precursor (YNU-2P) has been synthesized by a convenient SAC method. The structure of YNU-2P, which contains significant site defects, has been proposed by means of a modified Rietveld method. The defect sites have been successfully filled by vapor- or liquid-phase silylation and subsequent calcination. This silylation makes the calcined product YNU-2 (isomorphous to MCM-68) sufficiently stable to heat and converts the original YNU-2P into a purely siliceous microporous material. This result suggests that YNU-2P has great potential as a precursor for the positioning of various atoms in the framework, and the introduction of heteroatoms, such as Ti and Al, into the framework is currently being investigated.

Experimental Section

SDA: Dianion SA10A (OH) (Mitsubishi Chemical Co.) anion exchange resin (107 g, corresponding to 192 mmol of exchange capacity) was added to a solution of $TEBOP^{2+}(I^-)_2$ (22.0 g, 39.4 mmol) in water (200 mL) and the mixture was allowed to stand at room temperature for 47 h with occasional shaking. After filtration, the aqueous solution was concentrated to 73.6 g to give 0.507 mmol g^{-1} of $TEBOP^{2+}(OH^-)_2$ based on titration of the resulting solution. Yield: 95 %.

YNU-2P: In a typical procedure, the appropriate amount of NaOH was mixed with $TEBOP^{2+}(OH^-)_2$ solution and the mixture stirred for 10 min. Fumed silica (Cab-O-Sil M5, Cabot) was then added and stirring was continued for 3 h. The resultant gel was dried at 80 °C with continuous stirring. When the gel became thick and viscous, it was stirred with a Teflon rod until dry. The molar composition of the gel was $1.0\,SiO_2/0.1\,TEBOP^{2+}(OH^-)_2/0.15\,NaOH$. The dry gel was ground into a fine powder and this powder was poured into a small Teflon cup (20 mm ID × 20 mm), which was placed in a Teflon-lined autoclave (23 mL) containing water (the source of steam; approx. 0.2 g per gram of dry gel) in such a manner that the dry gel never comes into direct contact with the water. Crystallization of the dry gel was carried out at 150 °C under autogenous pressure for 5 days. After this time the autoclave was quenched with cold water and the crystalline material (YNU-2P) was removed from the cup, filtered, washed thoroughly with water, and dried overnight at room temperature.

YNU-2: Post-synthesis silylation was carried out before removal of the SDA from YNU-2P by calcination. This method consists of treating the as-synthesized sample (YNU-2P, 200 mg) with tetramethyl orthosilicate (TMOS, 24 mg, 158 mmol) vapor and conc. HCl (60 mg, 1.64 mmol) vapor inside the autoclave and heating statically at 170 °C for 24 h. The resultant crystalline solid was washed with water then calcined at 450 °C in air for 3 h.

The intensity data were collected at room temperature with a Bruker D8-Vario1 powder diffractometer in a modified Debye–Scherrer geometry using $Cu_{K\alpha 1}$ radiation from a primary monochromator. The experimental conditions used to collect the intensity data sets for each sample are summarized in Table 1. The diffractometer was equipped with a linear position-sensitive detector VÅNTEC-1 (8° 2θ) and was operated at 40 kV and 50 mA. The samples were sealed in borosilicate capillary tubes with an inner diameter of 0.5 mm. Refined structural and geometrical parameters for both

YNU-2P and YNU-2 are summarized in the Supporting Information. The solid-state ^{29}Si MAS NMR spectra (hpdec pulse sequence) were recorded at a spinning frequency of 5 kHz using a 7-mm MAS probe, a 30° pulse length of 1.6 μs, and a 100-s cycle delay time with a Bruker AVANCE 400 WB spectrometer at 79.495 MHz. The solid-state ^{1}H MAS NMR spectra were obtained with a spinning frequency of 16 kHz using a 4-mm MAS probe, a 90° pulse length of 4.0 μs, and a 4-s cycle delay time on the same spectrometer at 400.130 MHz. The ^{1}H and ^{29}Si chemical shifts were calibrated with a standard sample of tetramethylsilane. Thermogravimetric analysis was carried out with a MAC Science TG-DTA 2100SA in dry air at a heating rate of 10 °C min^{-1}. Nitrogen adsorption and desorption isotherms at −196 °C were measured with a BELSORP-max-1-N gas adsorption instrument (Bel Japan) for samples pre-treated at 400 °C for 2 h. The BET specific surface area (S_{BET}) was calculated from adsorption data in the relative pressure (P/P_0) range from 0.04 to 0.1. The external surface area was estimated by the *t*-plot method and the pore volumes were estimated mainly by the *t*-plot method in combination with the BJH method. FE-SEM images were recorded with a Hitachi S5200 microscope. Elemental analyses were performed by ICP (Shimadzu ICP-8000E).

Received: September 13, 2007
Published online: December 28, 2007

Keywords: crystal growth · silicates · structure elucidation · X-ray diffraction · zeolite analogues

[1] C. Baerlocher, L. B. McCusker, D. H. Olson, *Atlas of Zeolite Framework Types*, 6th ed., Elsevier, Amsterdam, **2007**; see also: http://www.iza-structure.org/databases/.
[2] D. L. Dorset, S. C. Weston, S. S. Dhingra, *J. Phys. Chem. B* **2006**, *110*, 2045 – 2050.
[3] D. C. Calabro, J. C. Cheng, R. A. Crane, Jr., C. T. Kresge, S. S. Dhingra, M. A. Steckel, D. L. Stern, S. C. Weston, U.S. Patent 6049018, **2000**.
[4] S. Ernst, S. P. Elangovan, M. Gerstner, M. Hartmann, S. Sauerbeck, *Abstr. 14th Int. Zeol. Conf.* **2004**, 982 – 983.
[5] S. P. Elangovan, M. Ogura, S. Ernst, M. Hartmann, S. Tontisirin, M. E. Davis, T. Okubo, *Microporous Mesoporous Mater.* **2006**, *96*, 210 – 215.
[6] T. Shibata, S. Suzuki, K. Komura, Y. Kubota, Y. Sugi, H. Kim, S. Gon, unpublished results.
[7] M. Matsukata, M. Ogura, T. Osaki, P. R. H. P. Rao, M. Nomura, E. Kikuchi, *Top. Catal.* **1999**, *9*, 77 – 92.
[8] A. Boultif, D. Louer, *J. Appl. Crystallogr.* **2004**, *37*, 724 – 731.
[9] F. Izumi, T. Ikeda, *Mater. Sci. Forum* **2000**, *321–324*, 198 – 203.
[10] C. Baerlocher, L. B. McCusker, L. Palatinus, *Z. Kristallogr.* **2007**, *222*, 47 – 53.
[11] L. Palatinus, G. Chapuis (**2006**): Superflip—computer program for solution of crystal structures by charge flipping in arbitrary dimensions; http:/superspace.epfl.ch/superflip.
[12] C. Baerlocher, F. Gramm, L. Massüger, L. B. McCusker, Z. He, S. Hovmöller, X. Zou, *Science* **2007**, *315*, 1113 – 1116.
[13] M. Takata, N. Nishibori, M. Sakata, *Z. Kristallogr.* **2001**, *216*, 71 – 86.
[14] F. Izumi, R. A. Dilanian in *Recent Research Developments in Physics*, *Vol. 3*, *Part II*, Transworld Research Network, Trivandrum, **2002**, pp. 699 – 726.
[15] F. Izumi, S. Kumazawa, T. Ikeda, T. Ida in *Powder Diffraction* (Ed.: S. P. Sen Gupta), Allied Publishers, New Delhi, **1998**, pp. 24 – 36.
[16] K. Momma, F. Izumi, *Commission on Crystallographic Computing IUCr Newsletter* **2006**, No. 7, pp. 106–119.
[17] H. Eckert, J. P. Yesinowski, L. A. Silver, E. M. Stolper, *J. Phys. Chem.* **1988**, *92*, 2055 – 2064.

